Tuning the polarized quantum phonon transmission in graphene nanoribbons

2015 Nanotechnology 26 305401

(http://iopscience.iop.org/0957-4484/26/30/305401)

IOP Publishing Nanotechnology
Nanotechnology 26 (2015) 305401 (6pp) doi:10.1088/0957-4484/26/30/305401

Tuning the polarized quantum phonon transmission in graphene nanoribbons

P Scuracchio[1,2], A Dobry[1,2], S Costamagna[2,3] and F M Peeters[3]

[1] Facultad de Ciencias Exactas Ingeniería y Agrimensura, Universidad Nacional de Rosario, Av. Pellegrini 250, S2000BTP Rosario, Argentina
[2] Instituto de Física Rosario, Bv. 27 de Febrero 210 bis, S2000EZO Rosario, Argentina
[3] Universiteit Antwerpen, Department of Physics, Groenenborgerlaan 171, 2020 Antwerpen, Belgium

E-mail: scuracchio@ifir-conicet.gov.ar

Received 15 March 2015
Accepted for publication 3 June 2015
Published 7 July 2015

Abstract

We propose systems that allow a tuning of the phonon transmission function $T(\omega)$ in graphene nanoribbons by using C^{13} isotope barriers, antidot structures, and distinct boundary conditions. Phonon modes are obtained by an interatomic fifth-nearest neighbor force-constant model (5NNFCM) and $T(\omega)$ is calculated using the non-equilibrium Green's function formalism. We show that by imposing partial fixed boundary conditions it is possible to restrict contributions of the in-plane phonon modes to $T(\omega)$ at low energy. On the contrary, the transmission functions of out-of-plane phonon modes can be diminished by proper antidot or isotope arrangements. In particular, we show that a periodic array of them leads to sharp dips in the transmission function at certain frequencies ω_ν which can be pre-defined as desired by controlling their relative distance and size. With this, we demonstrated that by adequate engineering it is possible to govern the magnitude of the ballistic transmission functions $T(\omega)$ in graphene nanoribbons. We discuss the implications of these results in the design of controlled thermal transport at the nanoscale as well as in the enhancement of thermo-electric features of graphene-based materials.

Keywords: graphene, heat transfer, phonons

(Some figures may appear in colour only in the online journal)

1. Introduction

Immediately after the first measurements of graphene's extraordinary large thermal conductivity [1–3], its vibrational properties have become an object of intense research [4–7]. The low density of states at the Fermi energy makes the contributions of free electrons (Dirac fermions) negligible [8] and the intrinsic mechanisms behind the outstanding thermal transport properties are then almost completely attributed to the phonon characteristics. These investigations, together with the improvements in fabrication techniques [9, 10], have demonstrated the high potential for using graphene in obtaining rapid thermal dissipation, a topic highly important for present and future nano-electronic devices [11]. Measurements of thermal transport in the ballistic limit, where the phonon mean-freepath is larger than the dimensions of the sample, have not been reached yet experimentally. Recent very promising works, however, have shown new insights of this limit [12–14]. Beyond the sample-size dependency [15], different arrangements of atomic vacancies, carbon isotopes, and distinct boundary conditions have also a strong impact on the phonon transport [16–21]. Some results of these effects were already known from studies on carbon nanotubes [22–24] and have been extended to graphene nanoribbons (GNRs) [18, 25]. In general, all these studies were focused mainly on the reduction of the total thermal conductivity leaving the microscopical details somehow unattended.

In this work, we demonstrate that it is possible to use adequate configurations of boundary conditions, antidot arrangements and isotopic barriers to tune the polarized ballistic phonon transmission in GNRs. We show that particular local atomic displacements can be controlled with the purpose of filtering incoming in-plane or out-of-plane phonon modes at specific energies. In adittion to the tuning of the phonon transmission function $T(\omega)$, our findings also have important consequences for related problems of high interest, including

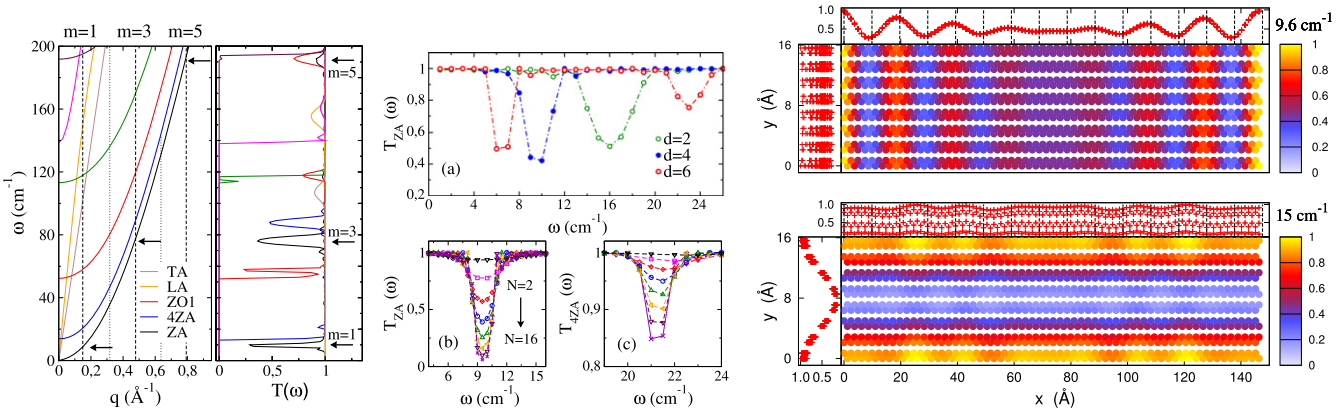

Figure 1. Isotopic barriers. Left: phonon relation dispersions of a free-edge homogeneous ZGNR and polarized transmission fucntions $T(\omega)$ for $N = 10$ isotopic barriers separated by $d = 4$. Center: (a) variation of $T_{ZA}(\omega)$ against the barrier distance $d = 2$, 4, 6 for $N = 8$. Dependence with $N = 2$, 4, …, 16 for the first dip of (b) $T_{ZA}(\omega)$ and (c) $T_{4ZA}(\omega)$ for $d = 4$. Right: LDOS profile at $\omega = 9.6$ (first dip) and 15 cm^{-1} for $N = 8$ and $d = 4$.

the search for enhanced thermoelectric behaviors [26] and the improvement of mechanical properties by controlled defect creation [27].

2. Method and model

Interactions between carbon atoms inside GNRs were modeled with a harmonic fifth-nearest neighbor force-constant model (5NNFCM). Parameters of the 5NNFCM account for the radial bond-stretching, in-plane and out-of-plane tangential bond-bending interactions [28]. This model has been proven to describe phonon dispersions and elastic constants of single and multi-layer graphene with excellent accuracy [29]. It was also used recently by us to investigate the role of single atomic vacancies and boundary conditions in the thermal transport properties of GNRs [30]. Here, we expand the study with special emphasis on the management of the polarized transmission functions.

Zigzag graphene nanoribbons (ZGNRs) were defined in the usual way respecting the hexagonal lattice and the edge-shapes at the boundaries. Definitions of free- and supported-edge boundary conditions and calculations of the contributions to $T(\omega)$ were performed using the formalism presented in [30]. The following systems are investigated in detail: (i) C^{13} isotopes were modeled by changing the atomic mass of carbon atoms keeping unaltered the magnitude of the forces; (ii) atomic vacancies were introduced by switching off the interatomic interactions with the missing atoms and (iii) partially supported-edges were defined by fixing certain carbon atoms outside the ribbon. Although not shown here, similar results were obtained for armchair GNRs.

In the absence of inhomogeneities, the phonon spectrum can be obtained by numerical diagonalization of the dynamical matrix [29]. The phonon spectrum of an homogeneous free-edge ZGNR contains four acoustical phonon modes, i.e. one extra acoustical mode as compared to bulk graphene. In the long wavelength regime the in-plane longitudinal (LA) and transversal (TA) modes exhibit linear energy dispersion, the out-of-plane (ZA) mode has quadratic dispersion and the so-called fourth acoustic (4ZA) mode possesses a linear energy dispersion [30]. Similar to what occurs in CNTs, as shown in figure 1 (left panel), this last mode has a small size-dependent energy gap when it is obtained using a force constant model [31–35]. At higher energies, out-of-plane (ZO-*n*th) and in-plane optic modes are present. For supported-edge ZGNRs, all phonon modes develop an energy gap due to the breakdown of the translational symmetry [30].

The calculation of the energy-dependent transmission function $T(\omega)$ was performed by using the non-equilibrium Green's function formalism within the conventional Landauer method [36, 37]. Anharmonic terms and electron-phonon interactions were neglected. As described elsewhere, the central region containing antidots, isotopes or supported-edge zones, was connected to two homogeneous semi-infinite contacts at different temperatures. Surface Green's functions (SGF) were calculated iteratively by using the decimation technique [38, 39]. The polarized incident components of $T(\omega)$ were identified by proper rotation of the SGF to the basis of normal phonon modes [40].

3. Results and discussion

3.1. Out-of-plane phonon modes

The quadratic phonon dispersion displayed by the out-of-plane ZA phonon mode at low energy entails important consequences in the temperature-dependent properties of the graphene lattice. For instance, the ZA mode is responsible for the subtle lattice thermal contraction which takes place at intermediate temperatures [41]. The smaller group velocity $\nu_n(\omega) = \partial\omega/\partial q$ of the out-of-plane mode (n = ZA) in the long wavelength regime as compared to the in-plane modes also have important effects on the phonon transport. Given a fixed wave-vector, in-plane and out-of-plane incident waves will propagate at different speeds. Consequently, they interact differently with any obstacle (atomic vacancies, carbon

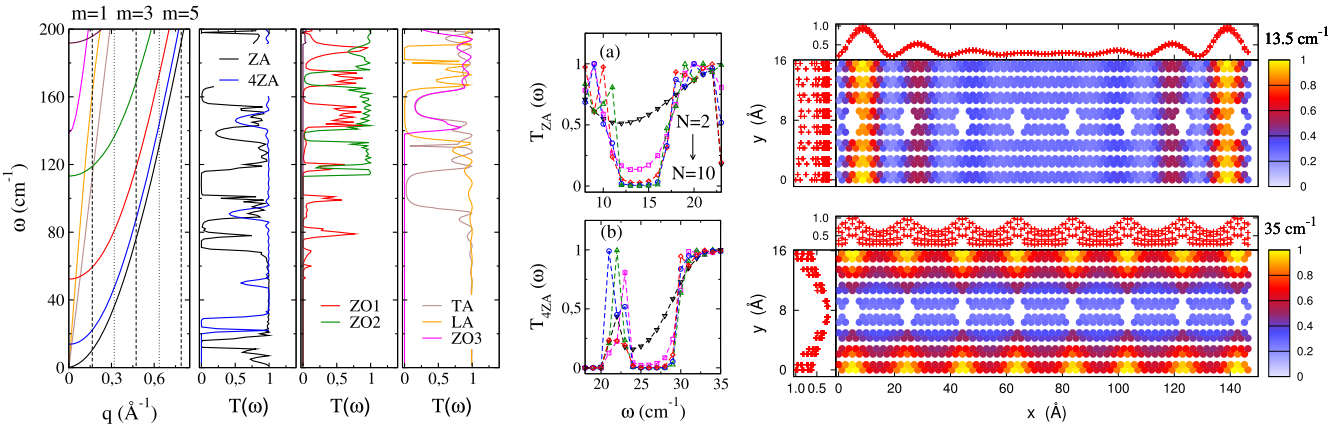

Figure 2. Antidot lattice. Left: phonon relation dispersions of a free-edge homogeneous ZGNR and $T(\omega)$ for $N = 10$ periodic antidots and $d = 4$. Center: Dependence with $N = 2, 4, \ldots, 10$ for the first dip of (a) $T_{ZA}(\omega)$ and (b) $T_{4ZA}(\omega)$ for $d = 4$. Right: LDOS profile at $\omega = 13.5$ (first dip) and 35.0 cm^{-1} for $N = 8$ and $d = 4$.

isotopes, any kind of impurity, etc) encountered on their way. If the obstacle is localized (extent limited to a small region in space) fast-moving waves will transit almost without being affected, but slow-moving waves will suffer partial reflection.

This effect can be more clearly seen in the analytical expression for the amplitude mode transmission $t_n^{RL}(\omega)$ obtained by using a mode-matching technique [42] in which $t_n^{RL}(\omega) = \mathrm{i}2\omega\{(E_R^+)^{-1}G_{N+1,0}[(E_L^-)^T]^{-1}\}_n \nu_n^L(\omega)$, where ν_n^L is the group velocity of the incident wave of mode n, $G_{N+1,0}$ is the corner element of the retarded Green's function for the junction part and E_R^+ and E_L^- are the matrices formed by the column eigenvectors for the reflected normal modes of the left and right leads, respectively. In the following we will show that by using specific configurations of isotope and antidot structures this phenomenon can be exploited in order to filter slow moving out-of-plane phonons at low energy.

We start by analyzing the effect of N finite periodic isotopic barriers positioned along the ZGNR. Each barrier consists of four consecutive columns of C^{13} isotopes, which are separated from each other by d columns of C^{12} atoms. The small mass variation (~8.34%) between C^{12} and C^{13} has a negligible impact on the thermal transmission when there are only a few random distributed isotopes (diluted limit). Only in case of large concentration of isotopes the thermal transmission becomes significantly distorted. In figure 1 (left panel) we show the low-energy behavior of $T(\omega)$ for $N = 10$ and $d = 4$. As observed, each single-phonon mode transmission presents a few visible dips. The energies at which these dips are present for each phonon mode n can be estimated as $\omega_m^n(q = m\pi/L)$ where m accounts for the mth dip, $L = (4 + d)\sqrt{3}a$ is the distance between isotopic barriers and $a = 1.42$ Å the bond length between carbon atoms. For a better comprehension we added arrows in order to identify the $m = 1$, 3 and 5 dips for the ZA mode on the plot. This situation resembles those for the transmission coefficients of weighted strings [43, 44]. Accordingly, the intensity of the dips is afffected by an extra modulation which depends on the barrier width [45]. In this particular case, the modulation produce a large attenuation of the $m = 2$ and 4 dips.

The shift of the first dip ($m = 1$) of $T_{ZA}(\omega)$ against the inter-barrier distance d is displayed in figure 1(a) (center). The estimated energies $\omega_1^{ZA} = 16.7$, 9.6 and 6.6 cm^{-1} for $d = 2$, 4, 6, respectively, are consistent with the values observed. In figures 1(b) and (c), we show the increasing intensity of the first dip of $T_{ZA}(\omega)$ and $T_{4ZA}(\omega)$ for increasing N, with fixed $d = 4$. Notice on the contrary that in-plane mode transmissions $T_{TA}(\omega)$ and $T_{LA}(\omega)$, remain unity (perfect transmission) up to large energies (109.1 and 158.6 cm^{-1}, respectively).

A better microscopic understanding of $T(\omega)$ is obtained by analyzing the local density of states (LDOS) of the atomic displacements, as shown in figure 1 (right panel). At $\omega = 9.6$ cm^{-1}, where the first dip of T_{ZA} appears, carbon atoms are confined to move between the first two closest barriers and the propagation of the incident wave is strongly inhibited. Observe that in the center of the periodic arrangement, LDOS is < 0.3. At a larger energy, $\omega = 15$ cm^{-1}, the incident wave exhibits almost perfect transmission through the set of barriers. Now, the active contribution of the edge-localized 4ZA mode produces larger displacements at both edges of the ribbon where the LDOS is approximately equal to one.

We now proceed with the analysis of $T(\omega)$ for a finite array of N periodic antidots. This kind of systems are currently of high interest due to their expected large thermoelectric characteristics [46–49]. Here, each antidot has been defined by eliminating a group of six carbon atoms and the distance between them is kept as in the case of isotopic barriers in order to obtain comparable behaviors.

In figure 2 (left panel) we show therefore the low-energy behavior of $T(\omega)$ for $d = 4$ and $N = 10$. Similarly as above, an overall analogous behavior with the gradual apparition of dips is found. Here, however, the antidot structure produces stronger perturbations in the atomic displacements and hence its effect on $T(\omega)$ is considerably larger. In figure 2 (center panel) it can be observed that by increasing N also here the intensity of dips becomes larger and already for $N = 8$ one gets $T_{ZA}(\omega)$ and $T_{4ZA}(\omega) \approx 0$ at the first dip. The LDOS corresponding to the first dip of the ZA mode at 13.5 cm^{-1} shown in figure 2 (right) shows again localized vibrations

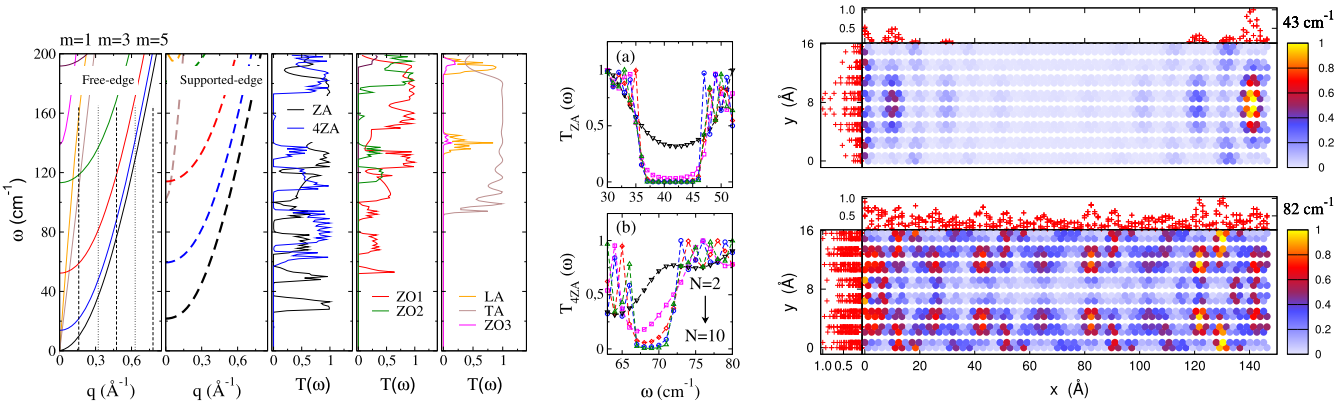

Figure 3. Partially supported edges. Left: phonon relation dispersions of a free- (continuous) and supported-edge (dashed lines) homogeneous ZGNR and $T(\omega)$ for $N = 10$ stripes and $d = 4$. Center: dependence with $N = 2, 4, \ldots, 10$ for the first dip of (a) $T_{ZA}(\omega)$ and (b) $T_{4ZA}(\omega)$ for $d = 4$. Right: LDOS profile at $\omega = 43.0$ (first dip) and 82.0 cm^{-1} for $N = 8$ and $d = 4$.

restricted to the area enclosed by the first set of antidots. Then, for $\omega = 35$ cm^{-1} where $T_{ZA} \approx 1$, the vibrational pattern is similar to the case analyzed previously where the 4ZA mode becomes active but there exists now an additional modulation of the displacements in the short direction of the ribbon due to the presence of the antidots.

3.2. In-plane phonon modes

In-plane LA and TA modes are characterized by their conventional acoustic linear dispersions at low energy. Their group velocities, estimated by using the 5NNFCM potential, are $\nu_{TA} = 14.3 \times 10^5$ cm s^{-1} and $\nu_{LA} = 23.1 \times 10^5$ cm s^{-1} for 2D graphene [29]. These values are relatively large when compared to other materials [50]. We show here that a more effective way of filtering these modes is, instead of using localized perturbations which only affect modes with low group velocity [42], by adopting partially supported edges. Within this setup, energy gaps at $q = 0$ are opened for all the phonon modes in the spectra. There are, however, differences in the magnitude of the gaps being significantly larger for the in-plane phonon modes as compared to the out-of-plane ones [30].

In what follows, we explore the effect of partially supported-edge ZGNRs on $T(\omega)$. The configuration considered consists of N periodic stripes, each of which consists of four columns of atoms where only those atoms lying at the edges are kept fixed. In this case a combined reduction effect for in-plane and out-of-plane transmissions is expected at low energy.

To facilitate the understanding of the results in figure 3 (left panel), we show also the phonon dispersion relations for an homogeneously supported-edge (dashed lines) ribbon, which displays the energy gaps [30] mentioned above, together with $T(\omega)$ for the case $N = 10$ and $d = 4$. The main difference is that now the transmission functions of the acoustical modes T_{ZA}, T_{LA}, T_{TA} and $T_{4ZA}(\omega)$ are zero until the energy of the incident waves reaches the values observed in figure 3 (left panel). These values are very close to the corresponding gaps of the first two out-of-plane modes and the first in-plane transversal mode of the supported-edge ZGNR. In this sense, note that while out-of-plane modes become active at relative small energies, $T_{TA}(\omega)$ and $T_{LA}(\omega)$ remain zero up to $\omega \sim 92$ and 133 cm^{-1}, respectively. The identification of dips produced by the periodic arrangement of stripes is now no longer simple as it was in the case of isotopic barriers. However, still now the first visible dips become more pronounced by increasing N for $T_{ZA}(\omega)$ and $T_{4ZA}(\omega)$ as can be observed in figure 3 (center panel).

Finally, in figure 3 (rightpanel) we show the LDOS at $\omega = 43$ and 82 cm^{-1} for $N = 8$ and $d = 4$. In the first case, the atomic displacements become gradually suppressed towards the center of the ribbon. Note also the nearby zero LDOS for edgeatoms at the supported parts of the ribbon. Then, for $\omega = 82$ cm^{-1} the situation is clearly more complex and the atomic displacements show traces of localization. Inside the supported-edge stripes, the LDOS displays the pattern of the second out-of-plane mode of supported-edge ZGNRs [30], while inside the free-edge stripes the LDOS shows a partial contribution of the 4ZA mode.

4. Conclusions

We have investigated the tuning of polarized ballistic thermal transmission functions in graphene nanoribbons by using different boundary conditions and proper arrangements of antidot structures and C^{13} isotopic barriers. We demonstrated that by adopting adequate configurations it is possible to tune the ballistic phonon transport by controlling the frequency and the magnitude of the transmission functions $T(\omega)$. When the width (W) of the GNR becomes larger, the energy gaps of the phonon modes at $\vec{q} = 0$ are expected to scale as $\sim$1/W and 1/W^2, for in-plane and out-of-plane modes, respectively [30]. Therefore, the overall trends are expected to remain valid.

In addition to the systems proposed here, similar effects could be achieved by other means such as by using proper configurations of adatoms like hydrogen [51], fluorine [52], etc. In the experimental setup, supported boundaries can be obtained in several ways. The ribbon could be deposited by

its edges over a substrate. In this case one expects van der Waals type interactions acting between distinct atoms and restricting the movement of edge-lying atoms. A good candidate with a very low lattice mismatch is h-BN [53, 54]. A stronger constriction can be obtained by adding a metallic material on top of the edges where covalent bonds are expected to form. Here, however, one may have extra contributions to the thermal transport from the free electrons in the metallic contacts.

Acknowledgments

Discussions with C E Repetto, C R Stia and K H Michel are gratefully acknowledged. This work was partially supported by the Flemish Science Foundation (FWO-Vl) and PIP 11220090100392 of CONICET (Argentina). We acknowledge funding from the FWO (Belgium)–MINCyT (Argentina) collaborative research project.

References

[1] Balandin A A, Ghosh S, Bao W, Calizo I, Teweldebrhan D, Miao F and Lau C N 2008 Superior thermal conductivity of single-layer graphene *Nano Lett.* **8** 902
[2] Seol J H *et al* 2010 Two-dimensional phonon transport in supported graphene *Science* **328** 213
[3] Ghosh S, Calizo I, Teweldebrhan D, Pokatilov E P, Nika D L, Balandin A A, Bao W, Miao F and Lau C N 2008 Extremely high thermal conductivity of graphene: Prospects for thermal management applications in nanoelectronic circuits *Appl. Phys. Lett.* **92** 151911
[4] Balandin A A 2011 Thermal properties of graphene and nanostructured carbon materials *Nat. Mater.* **10** 569
[5] Feng T and Ruan X 2014 Prediction of spectral phonon mean free path and thermal conductivity with applications to thermoelectrics and thermal management: a review *J. Nanomater.* 206370
[6] Balandin A A and Nika D L 2012 Phononics in low-dimensional materials *Mater. Today* **15** 266
[7] Nika D L and Balandin A A 2012 Two-dimensional phonon transport in graphene *J. Phys.: Condens. Matter* **24** 233203
[8] Novoselov K S, Geim A K, Morozov S, Jiang D, Zhang Y, Dubonos S, Grigoviera I and Firsov A 2004 Electric field effect in atomically thin carbon films *Science* **306** 666
[9] Yang X, Dou X, Rouhanipour A, Zhi L, Räder H J and Müllen K 2008 Two-dimensional grapheme nanoribbons *J. Am. Chem. Soc.* **130** 4216
[10] Cai J *et al* 2010 Atomically precise bottom-up fabrication of grapheme nanoribbons *Nature* **466** 470473
[11] Pop E, Varshney V and Roy A K 2012 Thermal properties of graphene: fundamentals and applications *MRS Bull.* **37** 1273
[12] Bae M H, Li Z, Aksamija Z, Martin P N, Xiong F, Ong Z Y, Knezevic I and Pop E 2013 Ballistic to diffusive crossover of heat flow in graphene ribbons *Nat. Commun.* **4** 1734
[13] Baringhaus J *et al* 2014 Exceptional ballistic transport in epitaxial graphene nanoribbons *Nature* **506** 349
[14] Bergfield J, Ratner M, Stafford C and di Ventra M 2015 Tunable quantum temperature oscillations in graphene nanostructures *Phys. Rev.* B **91** 125407
[15] Xu X *et al* 2014 Length-dependent thermal conductivity in suspended single-layer graphene *Nat. Commun.* **5** 3689
[16] Chen S, Wu Q, Mishra C, Kang J, Zhang H, Cho K, Cai W, Balandin A A and Ruoff R S 2012 Thermal conductivity of isotopically modified graphene *Nat. Mater.* **11** 203
[17] Hu J, Schiffli S, Vallabhaneni A, Ruan X and Chen Y P 2010 Tuning the thermal conductivity of graphene nanoribbons by edge passivation and isotope engineering: A molecular dynamics study *Appl. Phys. Lett.* **97** 133107
[18] Jiang J W, Wang B S and Wang J S 2011 First principle study of the thermal conductance in graphene nanoribbon with vacancy and substitutional silicon defects *Appl. Phys. Lett.* **98** 113114
[19] Zhang H, Lee G and Cho K 2011 Thermal transport in graphene and effects of vacancy defects *Phys. Rev.* B **84** 115460
[20] Haskins J, Kinaci A, Sevik C, Sevincli H, Cuniberti G and Cagim T 2011 Control of thermal and electronic transport in defect-engineered graphene nanoribbons *ACS Nano* **5** 3779
[21] Serov A Y, Ong Z and Pop E 2013 Effect of grain boundaries on thermal transport in graphene *Appl. Phys. Lett.* **102** 033104
[22] Saito R, Dresselhaus G and Dresselhouse M S 1998 *Physical Properties of Carbon Nanotubes* (London: Imperial College Press)
[23] Stoltz G, Mingo N and Mauri F 2009 Reducing the thermal conductivity of carbon nanotubes below the random isotope limit *Phys. Rev.* B **80** 113408
[24] Mingo N, Yang L, Han J and Anantram M P 2001 Resonant versus anti-resonant tunneling at carbon nanotube ABA heterostructures *Phys. Status Solidi* B **226** 79
[25] Scuracchio P and Dobry A 2013 Bending mode fluctuations and structural stability of graphene nanoribbons *Phys. Rev.* B **87** 165411
[26] Yuan S, Jin F, Roldán R, Jauho A and Katnelson M I 2013 Screening and collective modes in disordered graphene antidot lattices *Phys. Rev.* B **88** 195401
[27] Lopez-Polin G, Gomez-Navarro C, Parente V, Guinea F, Katsnelson M I, Perez-Murano F and Gomez-Herrero J 2014 Stiffening graphene by controlled defect creation arXiv:1406.2131v2
[28] Mohr M, Maultzsch J, Dobardzic E, Reich S, Milosevic I, Damnjanovic M, Bosak A, Krisch M and Thomsen C 2007 Phonon dispersion of graphite by inelastic x-ray scattering *Phys. Rev.* B **76** 035439
[29] Michel K H and Verberck B 2008 Theory of the evolution of phonon spectra and elastic constants from graphene to graphite *Phys. Rev.* B **78** 085424
[30] Scuracchio P, Costamagna S, Peeters F M and Dobry A 2014 Role of atomic vacancies and boundary conditions on ballistic thermal transport in graphene nanoribbons *Phys. Rev.* B **90** 035429
[31] Droth M and Burkard G 2011 Acoustic phonons and spin relaxation in graphene nanoribbons *Phys. Rev.* B **84** 155404
[32] Muñoz E, Lu J and Yakobson B I 2010 Ballistic thermal conductance of graphene ribbons *Nano Lett.* **10** 1652
[33] Huang Z, Fisher T S and Murthy J Y 2010 Simulation of phonon transmission through graphene and graphene nanoribbons with a Greens function method *J. Appl. Phys.* **108** 094319
[34] Yamada M, Yamakita Y and Ohno K 2008 Phonon dispersions of hydrogenated and dehydrogenated carbon nanoribbons *Phys. Rev.* B **77** 054302
[35] Gillen R, Mohr M, Thomsen C and Maultzsch J 2009 Vibrational properties of graphene nanoribbons by first-principles calculations *Phys. Rev.* B **80** 155418
[36] Zhang W, Fisher T S and Mingo N 2007 The atomistic Green's function method: an efficient simulation approach for nanoscale phonon transport *Numer. Heat Transfer* B **51** 333

[37] Wang J S, Agarwalla B K, Li H and Thingna J 2013 Nonequilibrium Green's function method for quantum thermal transport *Front. Phys.* **1** 2013
[38] Zhang W, Fisher T S and Mingo N 2007 *J. Heat Transfer* **129** 483
[39] Lopez Sancho M P, Lopez Sancho J M and Rubio J 1985 Highly convergent schemes for the calculation of bulk and surface Green functions *J. Phys. F: Met. Phys.* **15** 851
[40] Huang Z, Murthy J Y and Fisher T S 2011 Modeling of polarization-specific phonon transmission through interfaces *J. Heat Transfer* **133** 114502
[41] Mounet N and Marzari N 2005 First-principles determination of the structural, vibrational and thermodynamic properties of diamond, graphite, and derivatives *Phys. Rev.* B **71** 205214
[42] Wang J and Wang J S 2009 Single-mode phonon transmission in symmetry broken carbon nanotubes: role of phonon symmetries *J. Appl. Phys.* **105** 063509
[43] Griffiths D J and Taussig N F 1992 Scattering from a locally periodic potential *Am. J. Phys.* **60** 883
[44] Gomez B J, Repetto C E, Stia C R and Welti R 2007 Oscillations of a string with concentrated masses *Eur. J. Phys.* **28** 961
[45] Griffiths D J and Steinke C A 2001 Waves in locally periodic media *Am. J. Phys.* **69** 137
[46] Petersen R, Pedersen T G and Jauho A P 2011 Clar sextet analysis of triangular, rectangular and honeycomb graphene antidot lattices *ACS Nano* **5** 523
[47] Dvorak M, Oswald W and Wu Z 2013 Bandgap opening by patterning graphene *Sci. Rep.* **3** 2289
[48] Yan Y, Liang Q F, Zhao H, Wu C Q and Li B 2012 Thermoelectric properties of one-dimensional graphene antidot arrays *Phys. Lett.* A **376** 2425
[49] Chang P H, Bahramy M S, Nagaosa N and Nikolić B K 2014 Giant thermoelectric effect in graphene-based topological insulators with heavy adatoms and nanopores *Nano Lett.* **14** 3779
[50] Fultz B 2010 Vibrational thermodynamics of materials *Prog. Mater. Sci.* **55** 247
[51] Costamagna S, Neek-Amal M, Los J H and Peeters F M 2012 Thermal rippling behavior of graphane *Phys. Rev.* B **86** 041408 R
[52] Singh S K, Srinivasan S G, Neek-Amal M, Costamagna S, van Duin A C T and Peeters F M 2013 Thermal properties of fluorinated graphene *Phys. Rev.* B **87** 104114
[53] Singh S K, Neek-Amal M, Costamagna S and Peeters F M 2013 Thermomechanical properties of a single hexagonal boron nitride sheet *Phys. Rev.* B **87** 184106
[54] Woods C R *et al* 2014 Commensurate-incommensurate transition for graphene on hexagonal boron nitride *Nat. Phys.* **10** 451